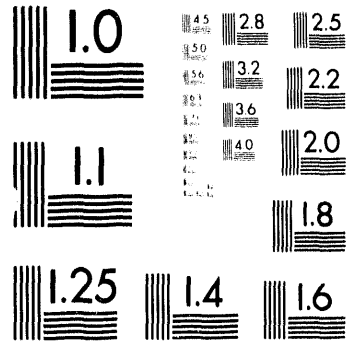
1.0
1.1
1.25
1.4
1.6
1.8
2.0
2.2
2.5
2.8
3.2
3.6
4.0
4.5
5.0
5.6

1 of 1

System design considerations for fast-neutron interrogation systems

B. J. Micklich, B. P. Curry, C. L. Fink, D. L. Smith and T. J. Yule
Engineering Physics Division, Argonne National Laboratory
9700 South Cass Avenue, Argonne, Illinois 60439 USA

ABSTRACT

Nonintrusive interrogation techniques that employ fast neutrons are of interest because of their sensitivity to light elements such as carbon, nitrogen, and oxygen. The primary requirement of a fast-neutron inspection system is to determine the value of atomic densities, or their ratios, over a volumetric grid superimposed on the object being interrogated. There are a wide variety of fast-neutron techniques that can provide this information. The differences between the various nuclear systems can be considered in light of the trade-offs relative to the performance requirements for each system's components (i.e., the source, target, detector array, and data processing). Given a set of performance criteria, the operational requirements of the proposed nuclear systems may also differ. For instance, resolution standards will drive scanning times and tomographic requirements, both of which vary for the different approaches.

We are modelling a number of the fast-neutron interrogation techniques currently under consideration, to include Fast Neutron Transmission Spectroscopy (FNTS), Pulsed Fast Neutron Analysis (PFNA), and its variant, 14-MeV Associated Particle Imaging (API). The goals of this effort are to determine the component requirements for each technique, identify trade-offs that system performance standards impose upon those component requirements, and assess the relative advantages and disadvantages of the different approaches. In determining the component requirements, we will consider how they are driven by system performance standards, such as image resolution, scanning time, and statistical uncertainty. In considering the trade-offs between system components, we concentrate primarily on those which are common to all approaches, for example: source characteristics versus detector array requirements. We will then use the analysis to propose some figures-of-merit that enable performance comparisons between the various fast-neutron systems under consideration. The status of this ongoing effort is presented.

1. INTRODUCTION

Nonintrusive interrogation techniques that employ fast neutrons are being studied to detect the presence of illicit substances, i.e., explosives and drugs, in luggage and cargo containers.[1] Fast-neutron techniques offer the possibility of determining the elemental densities, or their ratios, of several important light elements, such as carbon, oxygen, and nitrogen, based on their nuclear signatures. Explosives and drugs have unique nuclear signatures, as seen in Figure 1. Fast-neutron techniques are intended to complement existing techniques for illicit substance detection.

This paper first examines the four technical issues associated with any fast-neutron based system: (1) the fast-neutron source, (2) the nuclear signatures for the technique, (3) radiation detection, and (4) signal and image processing. Since our goal is to be able to evaluate the variety of fast-neutron techniques that are being proposed, we are developing the following tools required for these system studies. We are deriving simple analytical models to assess the ideal capabilities of a system. We are developing Monte Carlo simulation programs to look in more detail at the systems. Since each technique produces different types of signals that must be processed and analyzed, we are examining different signal processing algorithms and image processing approaches to detect illicit substances. Finally, we are developing tools that will allow the design of experiments to determine the real-world limitation of the techniques.

We have begun to apply our tools to the examination of two fast-neutron based systems. The first is based on detecting the neutron spectrum transmitted through the interrogated item; the technique is referred to in this paper as the Fast Neutron Transmission Spectroscopy (FNTS) technique.[2] The second is based on detecting gamma rays from neutron interactions in the material being interrogated; the technique is referred to as the Pulsed Fast Neutron Analysis (PFNA) technique.[3] We present some preliminary results of these studies. The ultimate goal of these studies is to determine the component requirements for each technique, identify tradeoffs imposed by system performance standards, and assess the advantages and limitations of the different techniques for various applications.

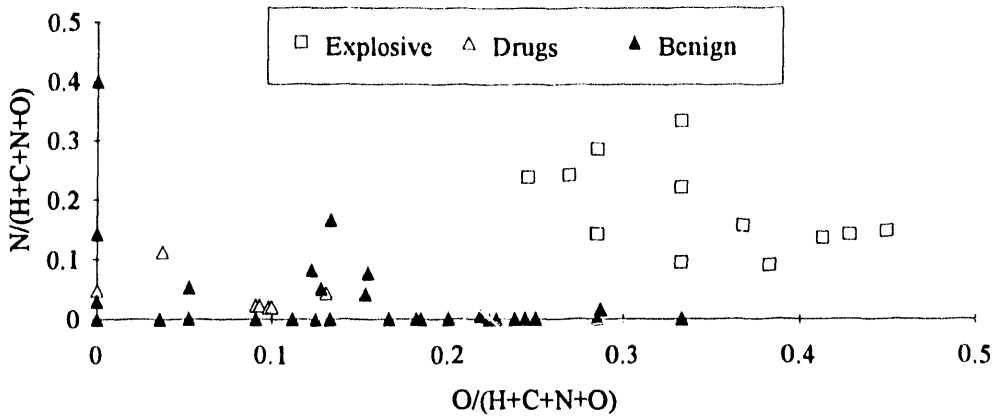

Figure 1. Two-dimensional representation of elemental compositions of explosives, drugs, and benign substances in terms of the normalized number densities of oxygen and nitrogen.

2. TECHNICAL ISSUES

2.1. Fast-neutron sources

Fast-neutron sources can either be monoenergetic, produced by thin-target beam interactions, or polyenergetic, with a neutron spectrum characteristic of the means of production (spontaneous fission, reactor, thick-target beam interaction, etc.). Accelerator-based sources have the advantage of being able to be turned off when not in use, and they can be pulsed to enable time-of-flight experiments or observation of capture or decay gamma radiation. Applications requiring intense neutron sources make use of protons or deuterons incident on low-Z targets such as lithium and beryllium. Measurements[4] of the source strength from the ^{9}Be(d,n) reaction (Figure 2) show that the yield increases rapidly with deuteron energy. The energy spectra also depend on deuteron energy, having relatively broad peaks with a sharp drop-off at $E_n \cong E_d$ - 1 MeV and small tails that extend to somewhat higher energies. For E_d = 5-6 MeV, the spectrum has a broad flat peak over the energy range 1-5 MeV, making it well suited for fast-neutron transmission measurements of elements with resonance structure in this energy regime.

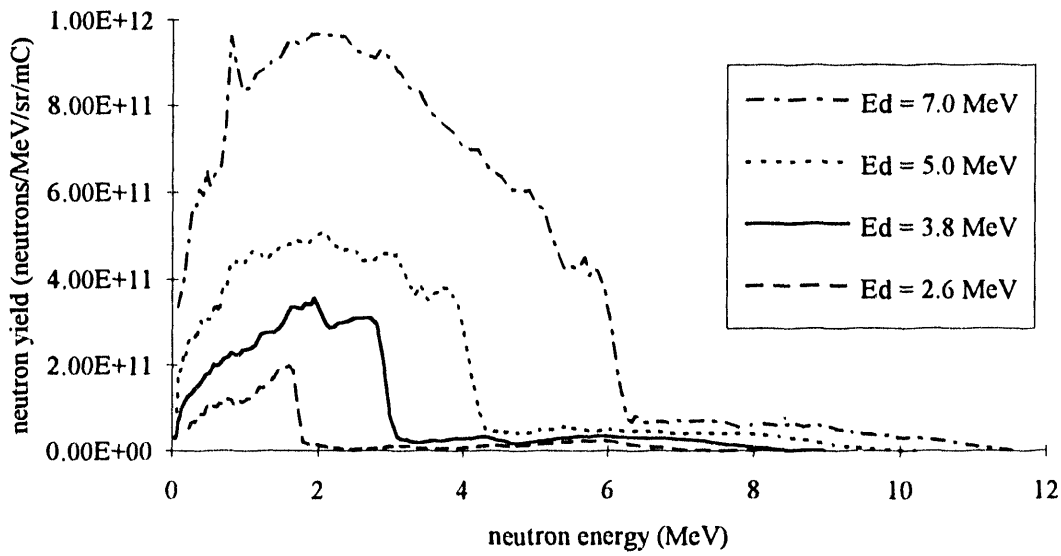

Figure 2. Neutron energy spectra from the ^{9}Be(d,n) reaction for different deuteron energies. The area under any curve is equal to the neutron yield at that energy.

One example of a monoenergetic source is the $^2H(d,n)^3He$ reaction in a thin gas target. The cross section and neutron energy as functions[5] of incident deuteron energy are shown in Figure 3. A typical application using 8-MeV neutrons would require deuterons with energy of approximately 5 MeV, where the cross section is about 60 mb/sr. The yield from this reaction depends on target design.[6] While a thicker target would give a greater yield, there would also be a loss of timing resolution in the neutron pulse due to the traversal time of the deuteron beam across the target and the difference between the neutron and deuteron velocities. For example, a deuteron with energy 5 MeV would take 4.5 nsec to traverse a gas target 10 cm long. Some spread in neutron energy may also be caused by deuteron-energy loss in crossing the target, depending on the gas pressure.

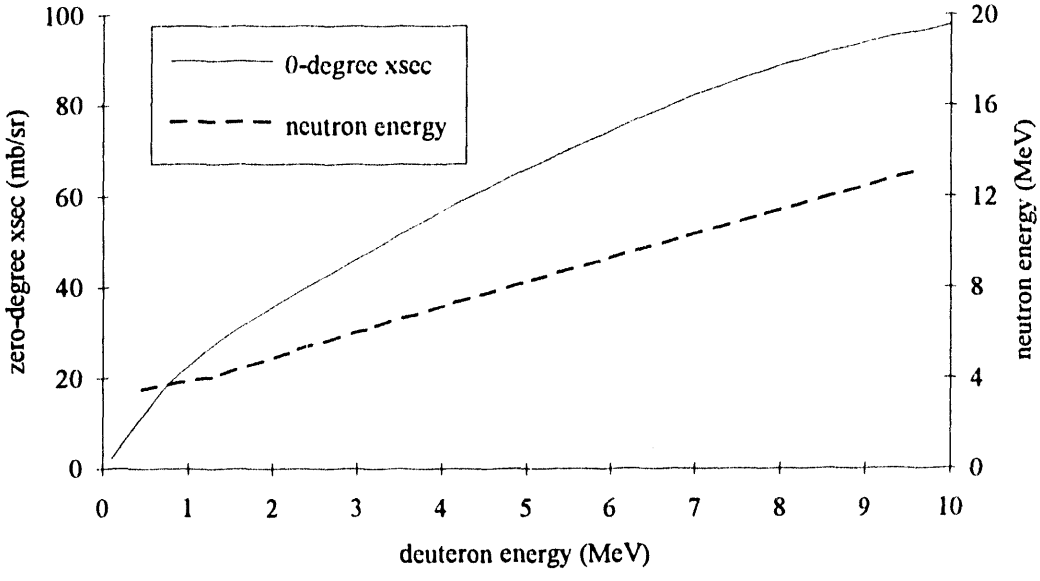

Figure 3. Zero-degree cross section and neutron energy for $^2H(d,n)^3He$ reaction.

Another monoenergetic source is based on the $^3H(d,n)^4He$ reaction. It has a larger cross section than the $^2H(d,n)$ reaction and can produce large numbers of 14-MeV neutrons at low incident energies. The relatively low incident energy leads to simpler source design, such as realized in sealed-tube neutron generators (STNG tubes) used in API. However, the interaction of these high-energy neutrons can yield complex gamma-ray spectra which can be difficult to interpret. Also, this reaction is not useful as a neutron source for transmission studies since there are no resonances near 14 MeV in light nuclei.

2.2. Nuclear signatures

Nuclear interrogation is governed by basic nuclear processes. We are interested in the "signatures" of these processes, in particular those initiated by neutrons. There are two detection categories, neutrons and gamma-rays. The relative importance of any process is determined by its cross section. It determines how many signature events can be expected for each incident neutron. Cross sections are determined from measurements and nuclear modeling. A useful information resource is the International Atomic Energy Agency document CINDA.[7] It is preferable to use evaluated cross sections, i.e., values recommended by experts who have examined available information from the literature. Several comprehensive national files are available. The best known is ENDF,[8] the U.S. file. Similar files are available from Western Europe (JEF file), Japan (JENDL file), Russia (Brond file) and China (CENDL file). The neutron energy range of interest is from thermal up to about 14 MeV for all technologies now under consideration. We are mainly concerned with fast neutrons (E_n > 100 keV). There are serious deficiencies in all these files that affect the quality of simulations that can be performed. For example, in ENDF several important total cross sections are inadequately known. The values for chlorine seem unphysical (see Fig. 4). Errors are missing for oxygen and nitrogen and they are large for carbon, iron, and copper.

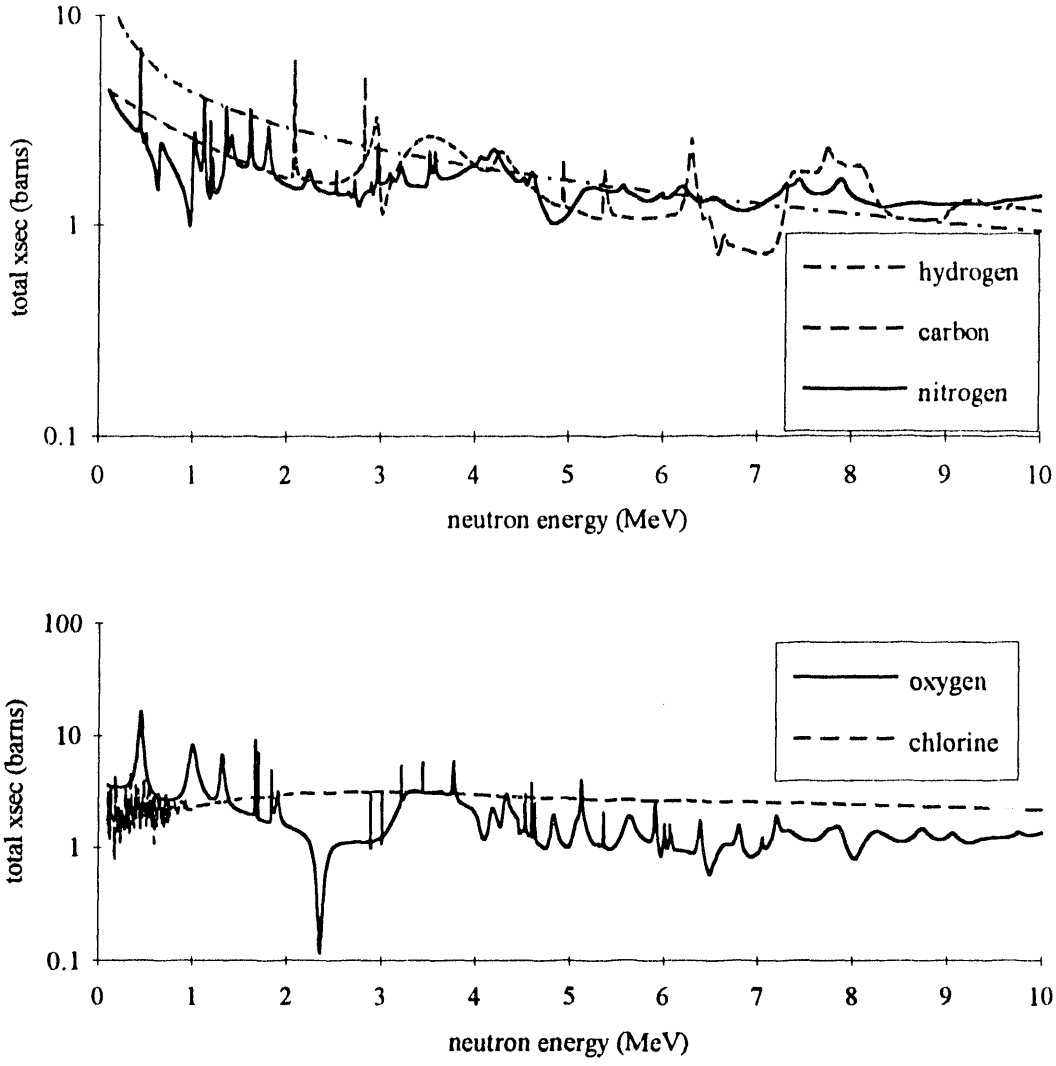

Figure 4. Total cross sections from ENDF/B-VI in the energy range 0.1 to 10 MeV for the elements hydrogen, carbon and nitrogen (top) and oxygen and chlorine (bottom).

Signatures based on neutron detection:

Total cross section: This cross section describes neutron removal from an incident beam passing through matter. For FNTS, the signature involves detecting non-interacting neutrons. Total cross sections tend to be a few barns, except at very low energies or in the vicinity of resonances.[9] Effective neutron removal cross sections are linear combinations of specific total cross sections, weighted by the elemental or isotopic densities. The total cross section is essentially devoid of structure for very light elements (i.e., H and He). Total cross sections of heavier elements exhibit characteristic resonance structure according to the partial reaction processes (e.g., elastic scattering, inelastic scattering, capture or transmutation reactions). Usually one considers only elemental cross sections because isotopic materials are not found in typical cargo packages. Total cross sections from 100 keV to 10 MeV for H, C, N, O and Cl appear in Fig. 4. The influence of the hydrogen total cross section can be significant. However, the unique amplitudes and shapes of specific resonances found in the heavier nuclei provide more readily detectable signatures for neutron transmission spectra. Consider the sharp solitary peak in carbon near 2.1 MeV, a similar peak in nitrogen near 330 keV and the dramatic dip found in oxygen near 2.4 MeV (Fig. 4).

Elastic and inelastic scattering cross section: The elastic and inelastic scattering processes tend to dominate in the keV-MeV range. The key to establishing a signature is neutron energy loss. Energy loss is only by kinematics in elastic scattering. This is significant for light targets and less so for heavier ones. Neutron scattering tends to be quite anisotropic (mainly forward-peaked) except at the lowest energies. Complicated diffraction patterns are observed at higher energies. Inelastic scattering involves a change of internal excitation of the target nucleus as well as kinematic losses. There is no inelastic signature for hydrogen. Carbon, nitrogen, oxygen and other heavier elements can be excited by inelastic scattering. The number of states available for few-MeV neutrons is limited in C, N and O (e.g., the first-excited state of ^{12}C is at 4.44 MeV[10]). Only neutrons with energies of several MeV can excite these elements. There is a tradeoff between having enough energy to provide yield and energies so high that the spectra are too complex. The signatures are thus very energy-dependent. There are rather severe constraints on the use of signatures from elastic and inelastic scattering for cargo interrogation. The incident neutrons must be monoenergetic and the object to be interrogated has to be thin. The desired signatures are very readily "washed out" by multiple scattering. The detectors and data recording system must provide a timing signal to yield an effective signature, even under ideal conditions.

Signatures based on gamma-ray detection:

Inelastic scattering: Neutron inelastic scattering provides more useful signatures when specific gamma rays are detected. Although gamma rays, like neutrons, are both scattered and absorbed in materials, gamma-ray signatures are more robust than those for neutrons. Incident neutron collimation and timing lead to signatures that tell us about the location as well as presence of certain elements. To produce usable signatures, incident neutrons must exceed the energy of the first-excited states. The cross section generally becomes adequate within a few hundred keV above threshold. Neutron energies of at least 5 MeV are needed to assay carbon by this method. For oxygen, the minimum is about 6.5 MeV. Nitrogen can be detected with neutron energies as low as 2.5 MeV. Inelastic gamma-ray production cross sections are rarely known to better than 20%; this and other factors limit the accuracy of elemental concentration determination. The signature quality also depends strongly on the neutron energy, cargo size, sharpness of timing signal and the chemical composition of the material. PFNA technology is based on neutron inelastic scattering.[11] API uses 14-MeV neutrons from the $^{3}H(d,n)^{4}He$ reaction. By detecting the alpha particle (^{4}He nucleus) associated with each neutron, one generates a timed and collimated neutron beam. The sensitivity is very low and 14-MeV neutrons produce very complex gamma-ray spectra in most materials. These spectra are very difficult to interpret.

Neutron capture: Neutron capture produces gamma-rays. There are strong signatures at very low energies or in the vicinity of specific resonances (e.g., the resonance region of cadmium). The cross sections are very small for MeV neutrons, so this process is of little interest in the present context. Spatial information is hard to obtain since most of the yield comes from primary neutrons that have been scattered many times before capture. The best known application of neutron capture interrogation involves observation of prompt gamma rays from ^{15}N produced by thermal neutron capture on ^{14}N. The technology developed from this concept is known as TNA.[12] In other techniques capture gammas constitute a source of background radiation.

Neutron transmutation reactions: Fast neutrons can induce more complex transmutation reactions in nuclei. For example, the $^{14}N(n,^{4}He)^{11}B$ reaction generates prompt gamma rays characteristic of ^{11}B. The $^{16}O(n,p)^{16}N$ reaction produces radioactive ^{16}N which decays to ^{16}O yielding characteristic gamma rays of this nucleus. The cross sections for these transmutation reactions are often smaller than for the other processes (except neutron capture) and they require fast neutrons. The possibilities for deriving spatial information from the interrogation are largely lost unless the gamma-rays are prompt.

2.3. Radiation detection

The conversion of the nuclear signature to a number requires that the signature interact within a detector, that the interaction produce a physical signal such as light, and that this light be converted to an electrical signal. This electrical signal is then processed to obtain information about characteristics of the signature to determine its validity before it is counted as an event. For example, in PFNA the signature of interest is the number of gamma rays at a particular energy and the origin of these gamma rays along the thickness of the container. The energy is obtained by integrating the light from the detector over a few microseconds and feeding this integrated signal, which is proportional to energy, to a counter that stores the

number of counts as a function of energy. The position information is obtained by doing time-of-flight between the interacting gamma ray and the accelerator pulse and correlating this position information with the energy information. In FNTS, the signature of interest is the neutron energy, which is obtained by time-of-flight.

The important characteristics of the detectors are the efficiency in detecting the nuclear signature, the amount of light produced by the signature interacting in the detector, and the decay time of the light output, which determines how accurately the timing can be measured in time-of-flight measurements. The characteristics of the signal processing system are its speed and accuracy in processing the electrical signal. Information on radiation detectors and signal processing can be found in Ref. 13.

For the energy range of neutrons being considered, the timing resolution of the neutron detector depends mainly on the thickness of the detector rather than the decay time of the light interaction. For a 2-MeV neutron and a timing resolution of 1 ns, the thickness should be on the order of 2 cm. The size of the photomultiplier affects the timing resolution because large photomultiplier tubes have poor timing resolution. Large photomultiplier tubes are also expensive. The typical efficiency for a 2-cm-thick neutron detector with a neutron threshold of 0.5 MeV is 20%, with a timing resolution of better than 1 nsec.

In general, gamma-ray detectors have a slower decay time than neutron detectors. However, this is not usually a limitation if one is also doing energy measurements at the same time, except in the case of large germanium detectors which have timing resolutions approximately a factor of 5 to 10 worse. A concern with gamma-ray detectors is obtaining both energy resolution and detection efficiency in the same detector at a reasonable cost. While the overall intrinsic efficiency (probability of detecting a gamma ray) is high, the probability of this detected gamma ray depositing all of its energy in the detector (photopeak fraction) is relatively small. For the inorganic NaI scintillator the intrinsic efficiency is approximately 60%, while the photofraction is 0.28 for a 10-cm diameter by 10-cm thick detector at 5 MeV. Thus the actual detector efficiency is approximately 17% for 5-MeV gamma rays. Other inorganic scintillators such as BGO and CaF_2 are becoming more widely used because of their better photopeak efficiency, but cost and energy resolution may limit their performance. Solid state germanium detectors have excellent energy resolution, but their efficiency is considerably worse than that of the inorganic detectors because of size limitations, especially as the energy of the gamma-ray increases.

2.4. Signal processing

The final component of the interrogation system is concerned with processing the signal produced by the detector into an indicator of the presence or absence of an illicit substance. This basically involves (1) correcting the measured counts for effects such as scattering or beam hardening, (2) converting the signal counts into a qualifier of the illicit substance such as number density, and (3) combining the signal with those from other detectors, other views, and possibly other interrogation techniques to determine the presence of illicit substances.

Corrections

Scattered radiation produces signals at the detector output that do not come from signatures originating in the interrogated voxel. The subject of scattering has not been seriously addressed in the various detection systems, especially those in which there are a large number of incident beams and/or detectors. The magnitude of the scattering impacts illicit substance detection in two ways. The first is due to the statistics of the detection process in which the error in the true signal is proportional to square root of the true signal plus the scattered signal. Thus, in large complex systems in which the transmission is less than a few percent, the scattered component must also be below a few percent. Even for relatively small systems in which the average transmission is typically 30 to 50%, scattering can be a problem because transmission through a book or other heavy object can be less than a few percent. Statistically, scattering can be overcome by increasing the data collection time, thereby increase the number of counts collected by the detector. The second effect of scattering is more important in systems which attempt to quantitatively determine the presence of illicit substances by directly measuring number densities. Scattering introduces a systematic uncertainty in the derived densities of the illicit substance, which can mask the differences between qualifiers for different substances. Other corrections, such as those for beam hardening and overall normalization, must also be considered. If these effects are dealt with inadequately, the fidelity of the qualifier is compromised and the reliability of substance identification suffers.

Qualifiers

The quantity that is measured experimentally in FNTS, PFNA, or x-ray techniques is the linear interaction coefficient, $\mu(j)$, where j refers to neutron or x-ray energy in the case of FNTS and x-ray techniques, and the gamma-ray energy in the case of PFNA. Detection of illicit substances uses these measured $\mu(j)$ to define a qualifier that separates illicit from benign substances. The term qualifier is used to refer to the functional relationship involving $\mu(j)$. The simplest qualifier is the value of $\mu(j)$ for a specific j. If there is more than one j value, then a qualifier could be defined that is some linear combination of the $\mu(j)$'s. A still more complicated qualifier is one that uses some combination of μ from a x-ray interrogation system and μ from a neutron interrogation system. Once a qualifier is chosen, then constraints are imposed on the subsequent system design requirements. The optimization and integration of qualifiers and system design constraints are areas of research that need to be expanded.

To quantify the concept of qualifier, consider a region of the container containing a compound J with an interaction coefficient μ, a compound density ρ, and molecular weights of the individual elements W_x and W_y. The linear attenuation coefficient for this region is

$$\mu(j) = \rho\left[\left(\frac{N_A}{A_X}\right)W_x\sigma_x(j) + \left(\frac{N_A}{A_Y}\right)W_y\sigma_y(j)\right] . \qquad (1)$$

where N_A is Avogadro's number, A_i is the atomic weight of element i, and $\sigma_i(j)$ is the interaction cross section, which is a function of the parameter j. The quantity $N_X = \rho\frac{N_A}{A_X}W_x$ is the atom density of the element x averaged over the region being interrogated.

The dependence of μ on the density of the compound is a significant problem in separating illicit and benign substances. A simple way to eliminate this density dependence is to measure μ for two different values of the parameter j, and to define a qualifier that is the ratio of these two μ's. Optimization of this qualifier in FNTS can be done by selecting the energies used. A different approach to eliminating ρ is to again measure μ at two different parameters of j and solve the linear set of equations for the number densities N_x and N_y. The quantities N_x and N_y are, in a sense, intermediate qualifiers, which still depend on density, but which provide some initial screening information. A linear combination of these number densities, however, defines a new qualifier that is independent of density. Note that while the ratio of the number densities is the simplest choice, other combinations could provide a better separation of illicit and benign materials.

A key assumption in the preceding development is that the region being interrogated contains only the compound of interest. In the case of mixtures of compounds, it is still possible to eliminate the density of the compound mixture, as in the case of a single compound, but now the qualifier will depend on the amount and type of the other compound. Thus it is important to keep the region being interrogated small. Since simple shadowgraph systems sample the entire thickness of the container being inspected, their sensitivity is limited by the presence of other compounds. This need to measure μ over a small volume to avoid the interfering effect of other compounds suggests that a multiple-view system will be required.

System Information

In an ideal world a single detector would produce a single qualifier that would indicate the presence or absence of an illicit substance. In the real world this is not possible, so one must obtain additional pieces of information and then process this additional information to determine the presence or absence of illicit materials. Since obtaining additional information will almost always lead to additional complexity and cost, it is in the interest of the system designer to minimize what is required without compromising the accuracy of the result. Exactly what additional information is needed has not really been explored even for a single qualifier. Two key questions are the volume resolution required and the number of projectional views of the inspected object that will be needed since they will have a significant impact on system cost and complexity. In

resolving these issues it is necessary to note that one is interested only in the binary question of whether an illicit substance is present. This is in some sense an easier question to answer than if one is interested in determining quantitative amounts. It should also be noted that the answer to the resolution and projection question is strongly tied to the qualifier chosen. Another question is whether the use of an x-ray scan could provide additional information that might reduce the number of neutron projections required. This is a useful question because the cost of x-ray systems is less than that for neutrons. This area of system integration needs the most attention in model development.

3. ANALYTICAL MODELS

Simple analytic models that use realistic assumptions about the radiation source, the source/detector geometry, and the interaction, detection, and analysis processes contribute physical insight into the issues surrounding candidate nuclear interrogation systems. These models give an important first look at concepts to determine whether or not further detailed investigation is warranted. Two such models are described below. One describes some statistical considerations in determining changes in the linear attenuation coefficient, and the other deals with some effects of detector count-rate limitations on system design.

3.1 Statistical considerations for required neutron fluence

In FNTS, the ultimate limit on image quality arises from the statistics of the counting process. Reference 14 shows that the neutron fluence Φ, in n/cm^2, required to detect a change δu in the linear attenuation coefficient μ within a small voxel of area δA and thickness δT is

$$\Phi = \frac{2\,SNR^2\, e^{\mu D}}{\left(\frac{\delta\mu}{\mu}\right)^2 (\mu\delta T)^2 (\delta A\,\varepsilon)} \left(\frac{1}{1-F}\right). \qquad (2)$$

Here D is the thickness of the object being inspected, ε is the efficiency of the neutron detector, SNR is the required signal-to-noise ratio, and (δT $\delta\mu$) is assumed to be less than 1. The scattering fraction F is given by $F = \frac{N_S}{N_U + N_S}$, where N_s is the number of scattered neutrons, and N_u is the number of neutrons transmitted. N_s and N_u are measured at the detector. Some typical numbers for fast-neutron interrogation of luggage are μ = 0.2 cm^{-1}, $\delta\mu$ = 0.1cm^{-1}, ε = 0.2, F = 0.5, D = 10 cm, and a required SNR of 5. Substituting these values into the above equation gives $\Phi = 3.6\cdot 10^5 / \left(\delta T^2 \delta A\right)$. Thus if δT is 1 cm and δA is 1 cm^2, the required neutron fluence is $3.6\cdot 10^5$. If the dimensions are reduced by a factor of ten, then the required flux is $3.6\cdot 10^9$. This inverse dependence of the fluence on the fourth power of the linear size of the volume usually limits the resolution available for reasonable source strengths.

Equation 2 is useful in determining parametric dependencies. For example, if F = 0, then the required fluence Φ is a minimum when μ is approximately 2/D, which corresponds to a transmission of 13.5%. If F is close to 1, however, the minimum fluence is obtained at μ = 1/D or 37% transmission. Note that this minimum in Φ is relatively broad. Equation 2 refers only to the effects of statistics on the image quality. Thus the effect of scattering from a statistical point of view is to increase the required incident flux. Systematic effects of scattering, however, can introduce uncertainties, which are significantly larger. Also, while an equation similar to Eqn. 2 holds for tomographic reconstruction[15], artifacts due to the reconstruction process can introduce larger uncertainties.

The required neutron flux for PFNA or similar systems can be derived in the same way as that of Eqn. 2. In this case the equation is given by

$$\Phi = \frac{SNR^2 e^{\mu_n L_1 + \mu_\gamma L_2}}{\left(\frac{\delta\mu_{\text{int}}}{\bar{\mu}}\right)(\bar{\mu}\delta T)(\delta A\,\varepsilon)(d\Omega/4\pi)}\left(\frac{1}{1-F}\right) \qquad (3)$$

Here, L_1 is the distance between the front of the system being inspected to the voxel being interrogated, and L_2 is the distance from the voxel to the exit of the container along the line of sight of the gamma-ray detector. The linear attenuation coefficient for the probing radiation reaching the voxel is μ_n, and the linear attenuation coefficient for the signature radiation leaving the system is μ_γ. The quantity $\delta\mu_{int}$ corresponds to the linear interaction coefficient for the production of gamma rays of interest, $\bar{\mu} = (\mu_n L_1 + \mu_\gamma L_2)/(L_1 + L_2)$, and $\delta\Omega/4\pi$ is the fraction of the solid angle subtended by the gamma-ray detector.

Equation 3 is similar to Eqn. 2 with the exception that $\delta\mu/\mu_{int}$ and $\mu\delta T$ are linear and not squared, and there is a dependence on the solid angle $\delta\Omega$. For the inelastic (n,n'γ) reaction with carbon to the 4.44-MeV level, a typical value for the cross section is 0.25 barns. Using a carbon density of $0.05 \cdot 10^{24}$ atoms/cm^3 gives a μ_{int} of 0.012 cm^{-1}. The solid-angle fraction of a typical gamma-ray detector (10 cm in diameter, approximately 50 cm from the target) is 0.0016. The value for $\bar{\mu}$ is similar to the μ for neutrons (0.2 cm^{-1}), and the photopeak efficiency of the gamma detector is approximately 0.17.

Finally, assuming that D is 10 cm and F is 0.5 gives $\Phi = 1.8 \cdot 10^8/(\delta T \delta A)$. For a volume of 1 cm^3 the incident flux requirements for PFNA will be approximately a factor of 300 times higher than for FNTS, while for a volume of 1 mm^3 the incident flux will be only 30 times higher. It should be noted that the increased flux requirements for PFNA can be offset to some extent by increasing the solid angle of the detector. Also, PFNA provides 3-dimensional information, which will require multiple projections with FNTS.

3.2 Implications of count-rate limits for system design

As an example of limitations imposed by detector constraints, consider a FNTS system for examining luggage. Typical system parameters may include an array of detectors each 10 cm in diameter at a source-detector distance of 500 cm, source and detector timing widths of 2 nsec, an average transmission of 0.3, and an average detector efficiency of 0.1. Under these conditions, neutrons in the energy range 0.5-10 MeV arrive at flight times of 100 to 500 nsec. A source repetition rate of at most 1 MHz should be used to avoid wrap-around. Assuming that each detector is limited to a counting rate of 10^5 n/sec, during the active period a detector can receive at most 40,000 counts each second, which would be the result of $40{,}000/(0.1)(0.3) = 1.33 \cdot 10^6$ neutrons emitted into the solid angle subtended by the detector. If the source is the ^{9}Be(d,n) reaction at E_d = 5 MeV, the source strength is $1.87 \cdot 10^{12}$ n/sr/mC, leading to an average current of 7 μA or a peak current of about 3.5 mA. This current would cause a peak heating in the target of 17.5 kW, with an average heating of 35 W.

Looking at these same figures another way, over a ten second period each detector would accumulate 400,000 counts distributed over roughly 200 time bins. If these counts are distributed uniformly, there would be 2000 counts per bin on the average. The uncertainty due purely to counting statistics would be on the order of 2.2%; the uncertainty will be greater when the effects of background, noise, scattering, etc., are included. Bins containing fewer than the average number of counts (i.e., corresponding to the high-energy tail) will have poorer statistics.

Models of this type indicate some interesting results. For example, if one moved the detector array back to a distance of 10 m to improve energy resolution, the detector solid angle would decrease by a factor of four and the range of neutron arrival times would be a factor of two longer. Thus one would need a source that was a factor of eight stronger to maintain the same detector count rates. However, the pulse repetition rate would have to be cut in half to avoid wrap-around (since the neutron flight times are twice as long) so that in a ten-second period only half as many counts would be accumulated. In

addition, both peak and average target heating would be higher. Moving the detectors in to 250 cm would reduce source strength requirements and allow a faster pulse repetition rate, but at a sacrifice in energy resolution.

4. MONTE CARLO SIMULATIONS

Following the application of simple models to investigate a candidate interrogation concept, subsequent analysis should treat more accurately the source characteristics, physics of the transport and interaction processes, detector efficiency, statistical uncertainties and noise in the detected signal, and the procedures for data analysis and substance identification. Monte Carlo transport codes such as MCNP,[16] which follow individual neutrons and photons from the source through the system to their detection, escape, or capture, are ideal for this type of analysis since they combine the simplicity, flexibility, and power needed to conduct investigations of basic physics questions surrounding candidate nuclear techniques. Insights to experiments and proof-of-principle systems are easily obtained since those changes (such as source strength or source/collimator/detector configurations) which make Monte Carlo statistics better (or worse) can be related to the corresponding measured quantities. In addition, the flexibility of Monte Carlo codes to specify sources, geometries, etc., allows the investigation of design tradeoffs for candidate systems far more easily, quickly, and inexpensively than an experimental design program.

Two approaches can be taken to modeling systems with Monte Carlo codes. One can attempt to predict the response of the system with the smallest fractional error by using an array of powerful variance reduction techniques such as the weight window and exponential transform. This is sometimes the only approach one can take, especially in optically thick media such as represented by cargo containers. An alternative is to use pure analog transport, in which each neutron from the source represents exactly one neutron from a real source in an experimental or test geometry. This is generally possible only in optically thin media, such as checked baggage. By incorporating realistic physical parameters, including detector efficiencies, one can arrive at results for which the fractional errors are equivalent to what one would expect in the real-world system. Having errors of the proper magnitude and variation across phase space is important in testing analysis and decision-making procedures that use the data. Some of the parameters involved in such an analysis can be predicted using analytic models, which allows an interplay between several of the tools described herein.

4.1 Fast-neutron transmission spectroscopy

Preliminary results have been obtained using MCNP to model a FNTS system. The neutron source is taken to be the forward-directed neutron energy spectrum from the ^{9}Be(d,n) reaction at E_d = 5 MeV (see Figure 2), with the time dependence a 2-nsec square wave. The source-detector distance is 500 cm, with the sample placed midway between in a tightly collimated geometry. Neutrons arriving at the detector are binned in 2-nsec wide intervals. Analog particle transport was used for these cases (i.e., no variance reduction). The number of histories was chosen using the analytic model of Section 3.2 to correspond to an irradiation time of ten seconds. An example of transmission ratios (the ratio of counts with the sample in to counts with no sample in each bin) for a typical explosive material (RDX) is given in Figure 5. The data for the time bins are analyzed for element areal density (nuclei/cm^2) using standard nuclear analysis techniques[17] adapted to the method of effective variance,[18] as described in Section 5. The cross section data used in the inversion procedure were obtained by modelling transmission experiments, choosing an average transmission of 0.3 to minimize errors in the calculated cross sections.[19] Elemental concentrations are expressed in terms of ratios, since in a transmission measurement of this type the sample thickness would not be known, so that one could not determine the absolute number densities of the elements.

An example of these results in terms of the qualifiers N/[H+C+N+O] and O/[H+C+N+O] is shown in Figure 6. These qualifiers are chosen since almost all common materials encountered in these investigations will have at least one of these elements, so that the chance of getting a zero denominator is small. This set of qualifiers also showed good discrimination between explosives, drugs, and benign materials (see Figure 1). Figure 6(a) shows the results of a number of repeated calculations of neutron transmission for the same material and thickness in order to investigate the reproducibility of the inversion scheme. Included in this figure are the 1-σ curves for each analyzed point. These curves show the locations of points that lie one standard deviation away from the center. These data show that the inversion scheme is robust in the sense that the qualifiers for all the data sets lie close to the true point. Figure 6(b) shows the 1-σ curves for different thicknesses of the sample, with all the calculated ratios again being close to the true values. The 1-σ curves initially get smaller as the transmission approaches the range 0.1-0.3, and then get larger as the transmission is further reduced.

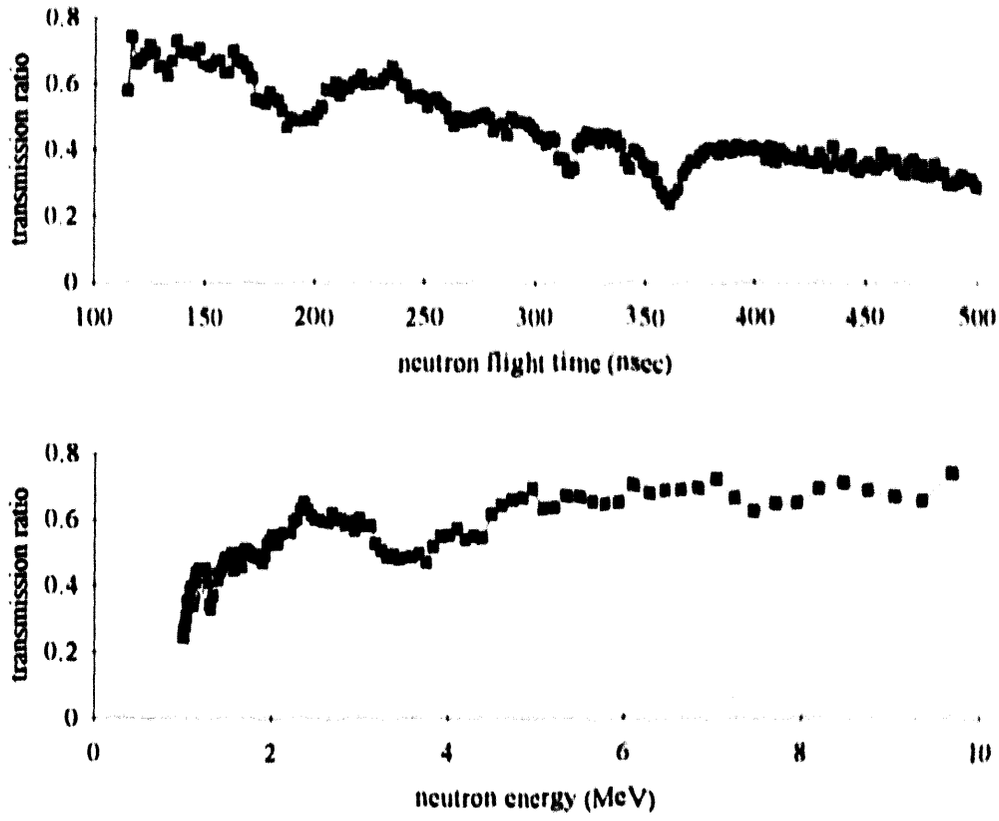

Figure 5. Fast neutron transmission through 3 cm RDX calculated with MCNP, shown in the time domain (top) and the energy domain (bottom).

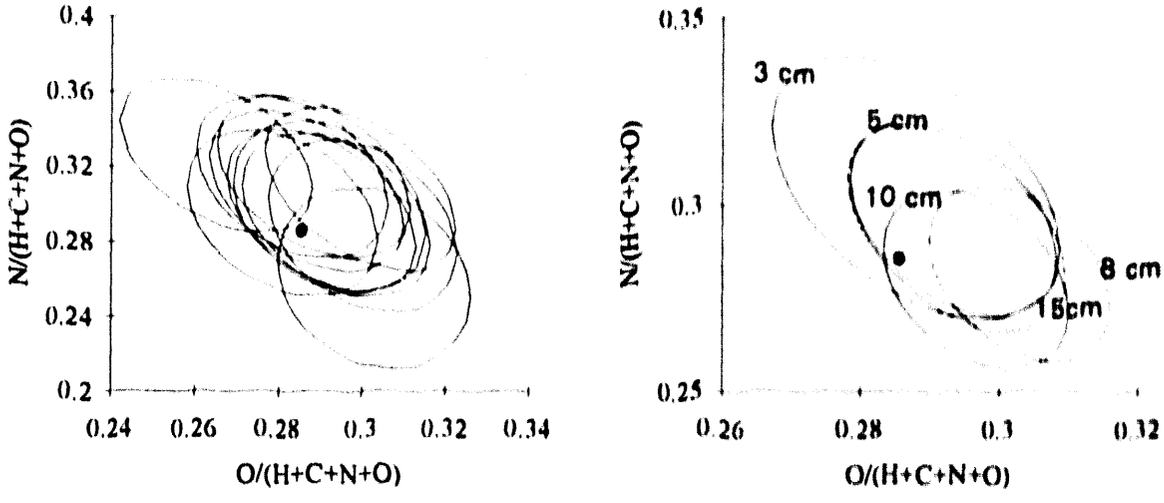

Figure 6. (a) 1-σ plots for a number of repeated independent calculations of fast-neutron transmission through 3 cm RDX (b) 1-σ plots for fast-neutron transmission through varied thicknesses of RDX. The 1-σ plot shows the curve of points located one standard deviation from the center. The probability that the point is contained within a 1-σ curve is 39.3%, for a 2-σ curve (not shown) the probability is 86.5%.

4.2 Pulsed fast-neutron analysis

The results presented for FNTS were for a tightly collimated geometry, so that scattered neutrons were not included. Some effects of neutron scattering are examined here for the case of PFNA, which has been described above. In this technique, localization of information about elemental concentrations is provided in directions transverse to the beam by source collimation. Localization along the beam direction is obtained by timing the total flight times of a source neutron and a detected gamma ray from inelastic scattering. For this timing to be possible, the inelastic events would have to occur only along the beam axis. The effect of neutron scattering would be to scatter high-energy neutrons out of the beam axis, so that gamma-ray signals might originate from other regions of the sample being interrogated.

Several MCNP cases were run for a 50-cm radius cylinder consisting of a single bulk material. The cylinder was 78 cm long, which corresponds to a 20-nsec flight time for 8 MeV neutrons. Neutrons were injected at one end along the cylinder axis. The cylinder was subdivided into ten 7.8-cm slices (2-nsec flight time), and the inelastic scattering rates from low-level excited states of carbon, nitrogen, and oxygen were tallied in each slice and in 2-nsec wide time bins. With the tally bins set up in this way, the source neutrons would be in the first slice during the first time bin, in the second slice during the second time bin, etc. Thus for proper timing of the neutron + gamma-ray paths, the inelastic gamma signal should be highest in the first slice during the first time bin, highest in the fifth slice during the fifth time bin, and so on.

Figure 7 shows the inelastic scattering rate for $^{12}C(n,n_1)$ (4.44-MeV level) vs. depth into the cylinder and for times between 12 and 20 nsec. Data for $^{16}O(n,n_2)$ (6.13-MeV level) are shown in Figure 8. If we examine the central core of radius 10 cm, we see that the inelastic scattering rate, and hence the inelastic gamma rate, peaks in the last slice of the cylinder as desired. However, if one looks at the entire cylinder, the inelastic scattering rate peaks at a shallower depth than desired, which would not preserve the timing accuracy required for imaging. This indicates that collimated detectors, on the opposite face of the sample from the source, may be required to preserve the proper timing information. The reduced count rate for the collimated detector would actually help since the gamma rays being rejected would be those originating in parts of the sample that are not being interrogated, and would just be contributing background and noise. These inelastic events are created by neutrons that scatter out of the incident beam and traverse the material at an angle, so that they do not penetrate to the same depth in a given time as those which remain in the incident beam.

Another point of interest is that the desired peaking is preserved better for oxygen that for carbon, for both collimated and uncollimated signals. This is a direct result of the relationship between the incident energy and the threshold energy for inelastic scatter. Since the threshold energy is farther below the incident energy for carbon, neutrons can experience more scattering events, suffering greater departures from the incident direction, and still retain sufficient energy to undergo inelastic scattering from carbon but not from oxygen. Inelastic scattering results from nitrogen (not shown here) support this conclusion. The inelastic scattering rate from a particular level is better correlated with the incident neutron "wavefront" for higher-energy excited states. Gammas resulting from the excitation of the first (2.31 MeV) and second (3.98) excited states in nitrogen may not be able to provide the proper timing information. On the other hand, the 0.72-MeV gamma that results from a transition between the sixth (5.83 MeV) and fourth (5.11 MeV) excited states in nitrogen could provide better timing information because of the higher threshold energy. Detection could be problematic for an element like chlorine, which has many low-level excited states lying close together.

Reduction of the incident neutron energy to 7 MeV would result in a large loss of signal for oxygen, and would only marginally improve timing for carbon and nitrogen. A higher neutron energy, such as that provided by the $^3H(d,n)$ reaction (14 MeV), would not only lead to more complex gamma spectra but would also involve more neutron scattering before passing the inelastic thresholds. On the whole, 8 MeV appears to be a nearly ideal choice for incident energy.

5. SIGNAL AND IMAGE PROCESSING

This section is concerned with how to make decisions about the presence of illicit substances from neutron interrogation of luggage and cargo. Characteristics of the subsystems and algorithms used to process the measurements depend on the type of measurements and choice of qualifiers; however, the approach developed to test various detection schemes must be general enough to apply to all the choices being considered. For example, the signal processing requirements for PFNA do

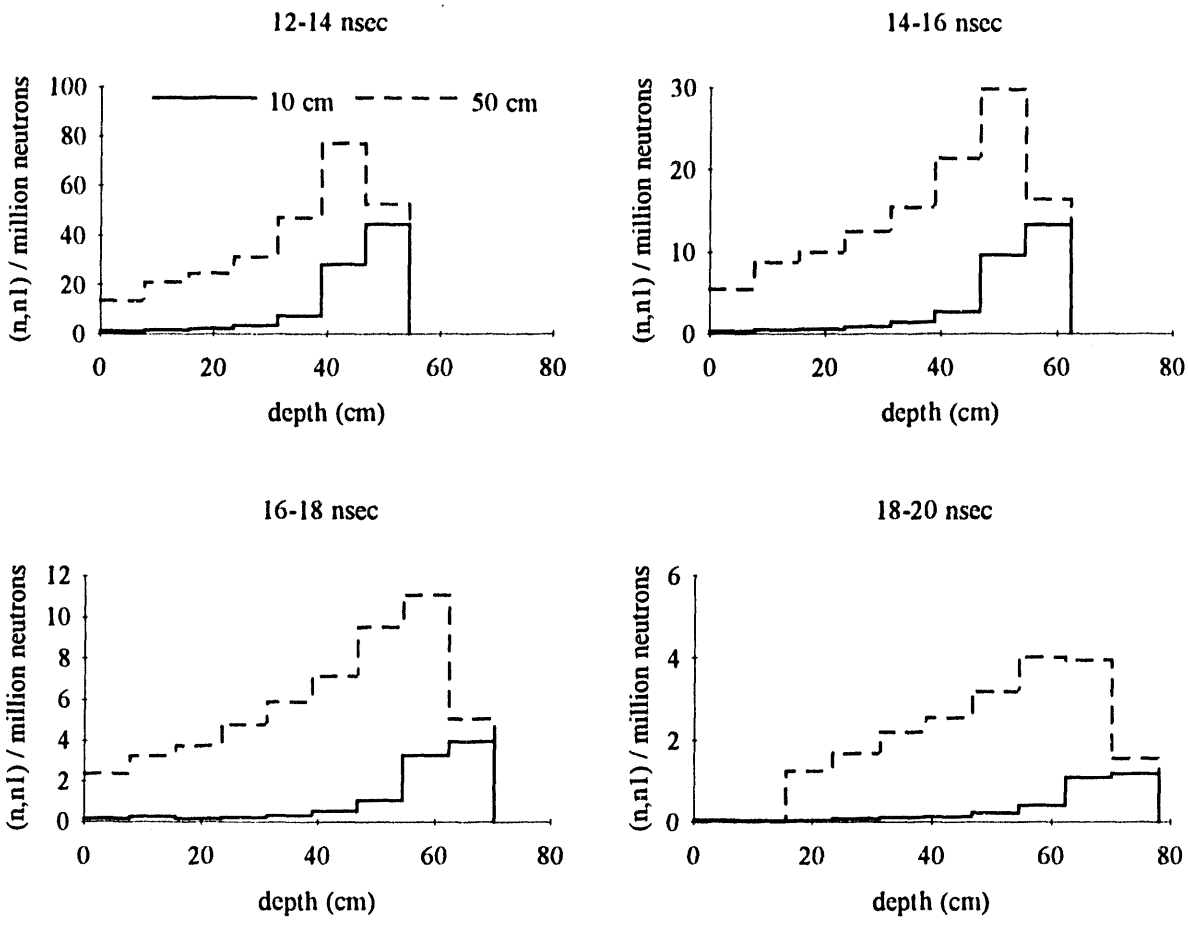

Figure 7. Inelastic scattering rate to first excited state (4.44-MeV) level of ^{12}C in a sugar sample as a function of position and of time. The solid line represents scattering rate (per million incident neutrons) in the central 10-cm radial core, and the dashed line represents the scattering rate in the entire (50-cm radius) sample. The four graphs show 2-nsec time slices from 12 to 20 nsec.

not include a tomographic step, because (in the absence of additional scattering) detection of the gamma ray produced in the primary interaction provides localization information.

A simplified flow chart for illicit substance detection based on FNTS is shown in Figure 9. Here, it is assumed that the projected species densities or species qualifiers are first determined and then the spatial distributions of these quantities are obtained by tomography. This order is not necessarily the optimum order in which to perform the processing. For example, one might prefer to perform tomography on projected linear attenuation coefficients measured at a few discrete neutron energies and then obtain qualifiers for a few suspicious volumes. Thus, one function for the tools discussed in this section is to test which order is optimum for signal and image processing from the stand point of accuracy of the final results.

For illicit substance detection schemes based on neutron transmission, one must develop and test both algorithms to map measured attenuation coefficients along a few lines of sight to areal densities (or qualifiers constructed from these densities) and image reconstruction algorithms that can perform tomography with a few projections. The effectiveness of the substance detection scheme must be tested under conditions that include effects of scattered neutrons. For schemes based on inelastic scattering with detection of the emitted gamma rays, with or without simultaneous detection of the scattered neutron, one's tools must be able to test the effect on the results of gamma rays originating within the voxel under interrogation and gamma rays produced outside the voxel but scattered into the detector.

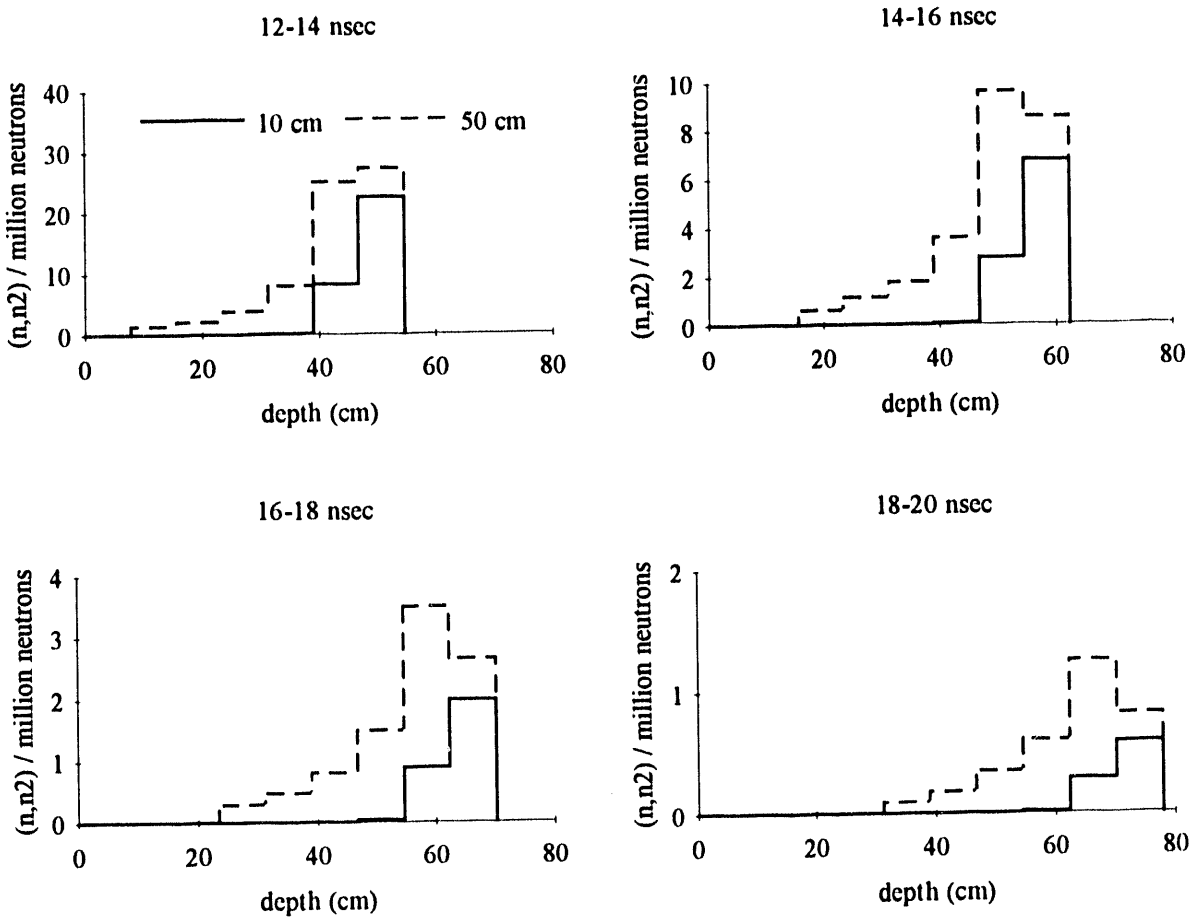

Figure 8. Inelastic scattering rate to second excited state (6.13-MeV) level of ^{16}O in a sugar sample as a function of depth and of time. The solid line represents scattering rate (per million incident neutrons) in the central 10-cm radial core, and the dashed line represents the scattering rate in the entire (50-cm radius) sample. The four graphs show 2-nsec time slices from 12 to 20 nsec.

The basic FNTS data are transmission measurements along lines of sight. From these measurements, the basic signal processing algorithms mentioned in Section 2.4 yield linear attenuation coefficients, which are functions of neutron energy, elemental species densities and species atomic numbers. Mapping of these results to areal species densities or qualifiers is accomplished by least-squares inversion algorithms. In addition to areal species densities, these algorithms yield covariance information from which one can construct confidence limits for the densities. Qualifiers can then be computed from the areal densities. Figure 6 shows typical results of inverting Monte Carlo simulated transmission data with our current species inversion algorithm.[20] This algorithm is based on procedures that were developed for earlier nuclear data programs.[17] Since both the measured linear attenuation coefficients and the cross sections used to invert areal species densities from these data have uncertainties, the inversion process is based on minimization of the effective variance.[18] Questions to be investigated with this and related tools include (1) effect of scattering on the uncertainties of the areal densities, (2) choice of inversion inputs to minimize vulnerability to systematic errors, and (3) efficacy of constrained linear inversion algorithms.[21] Addition of a trial function constraint to the present inversion algorithm would yield a related tool to permit testing whether the qualifier mapping procedure would benefit from using an initial trial function based, for example, on a homogenized distribution of substances expected in a typical piece of luggage or cargo. Other constraints (e.g., positivity) could also be implemented. Previous experience in another field has shown that iterative constrained

inversion techniques can be implemented in such a manner as to minimize the dependence of the results on the initial trial function,[22] and the proposed modification of the current inversion algorithm would be similarly implemented.

The spatial distribution of suspicious substances is determined by a reconstruction scheme similar to industrial tomography.[23] Computed Tomography (CT) involves constructing image slices of a three-dimensional object from a series of one-dimensional projections obtained from multiple line-of-sight transmission measurements. Medical tomography demands resolution on the order of 1 mm but such high resolution for a substance detection scheme may not be necessary. Typically, resolution on the order of 1 cm should be adequate for substance detection. Consequently, tomography algorithms capable of testing the use of few projections should be developed, and the relation between the number of views, the choice of substance qualifiers, and the accuracy of the final decision call (illicit substance present or absent in a particular voxel) should be tested with these tools.

Crewe and Crewe showed that as few as four views are sufficient for inexact tomographic reconstruction[24] if the areal species density maps or substance qualifier maps can be reduced to binary arrays. Specifically, they showed that a matrix of binary numbers can be reconstructed to sufficient accuracy from four projections: vector sums along the horizontal, vertical, and two principal diagonal directions. They also showed that the error in the reconstruction saturates at about 25% as the size of the matrix increases. Later, they constructed tomographic images of a hemoglobin molecule from scanning electron microscopic measurements along the three orthogonal view directions plus a fourth view at 45 degrees with respect to the two horizontal view directions.[25] The data were reduced to a 32x32 array of binary numbers for each 2-dimensional view; thus, the volume of the entire object was represented by 32^3 locations Each horizontal row of data in the four views was taken to represent a slice of the molecule projected onto the appropriate plane, and the reconstruction algorithm of their previous paper was employed. Similar image reconstruction algorithms should be constructed to test whether three or four views are sufficient for substance detection tomography. Inputs to these algorithms would be binary maps of qualifiers (on or off) projected on planes determined by the directions of the transmission lines of sight.

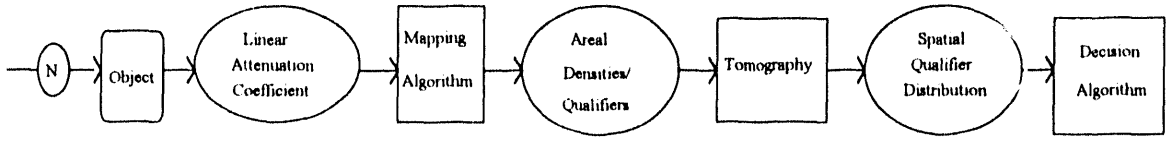

Figure 9. Flow Chart for an Illicit Substance Detection Scheme based on Neutron Transmission Measurements

6. EXPERIMENTS

The use of deterministic models and/or Monte Carlo simulation is an effective way to assess a concept's viability and to spot strengths and weaknesses. Still, there is a need to benchmark such studies with selective experiments. This does not require building a full-scale prototype system. Rather, certain critical aspects of the system ought to be mocked up and tested by measurements that are realistic but focused on specific issues.

First, no computational model can ever incorporate all the minute features of a physical system. Practical models focus on the key issues and overlook others. Otherwise, model parameterizations would be excessively cumbersome and computation times so long that one would not be able to learn about the critical features of the system in a reasonable amount of time. Nevertheless, certain details can be important. If key features of the model are missing the results can be misleading. Experiments designed to test the behavior of the system at critical junctures in the development process can give the necessary feedback to avoid serious mistakes. Another feature of experiments is that they provide calibration of a method's sensitivity. While numerical analysis gives such information too, the results are wholly dependent upon validity of the parameters introduced and the way they are used. Due to parameter uncertainties and method deficiencies, the true sensitivity of a concept may diverge considerably from calculated values. As an example, we can turn to reactor physics where clean benchmark critical assemblies are used to validate reactor calculations. The criticality constant and the true neutron spectrum can be determined experimentally and compared with Monte Carlo or deterministic transport calculations.

Benchmarking experiments are relatively inexpensive and can often be carried out on existing facilities, for example research accelerator facilities found at universities or national laboratories. Such a study is the work of Overley and coworkers on the neutron transmission technique to measure elemental concentrations.[26] A collimated beam of neutrons produced by ^{9}Be(d,n) reactions is transmitted through various materials. Time-of-flight techniques are employed to provide energy sensitivity, and the data lead to knowledge of H, C, N and O in the samples. These experiments provide a good test of the total cross section data base and show how such considerations as the primary neutron source spectrum and its intensity impact on statistical accuracies that can be obtained in practice. The impact of timing resolution is also reflected in these data in a manner that is possible to demonstrate only approximately by simulations. A similar approach appears in the work by Sawa and coworkers.[11] These experiments measure C, N and O content of materials by detecting gamma rays from nuclei excited by neutron inelastic scattering. Spatial information is derived by using pulsed neutrons and associated timing signals.

7. CONCLUSIONS

Our examination of the technical issues (fast-neutron sources, nuclear signatures, radiation detection, and signal and image processing) has shown that there are many tradeoffs that will be involved in the design of a useful fast-neutron based interrogation system. Any system will possess not only a set of capabilities, but also a set of limitations. We have begun the development of a set of tools to determine these for proposed systems. Simple analytical models are valuable for performing scoping calculations. Detailed modelling based on Monte Carlo simulations is needed because realistic analysis of a system involves complex neutron and gamma-ray transport considerations. The viability of a system is very dependent on the success of the signal and image processing approaches. For most systems, this is one of the most technically challenging areas. We conclude that it will often be necessary to do benchmark experiments before committing to the construction of a costly, complete system. Our preliminary analyses of two representative fast-neutron based systems, FNTS and PFNA, have shown the need for a comprehensive set of tools if one is to correctly assess the advantages and limitations of different systems for various applications.

8. ACKNOWLEDGMENTS

The help of Adrienne Novick and Michael Harper in implementing the FNTS species unfolding algorithm and analyzing the results from Monte Carlo calculations is gratefully acknowledged. Michael Harper was supported as a Summer Student Research Participant by Argonne's Division of Educational Programs. Inspiration and many fruitful ideas were gained from discussions with Bart Clare and Ron Martin.

9. REFERENCES

1. T. Gozani, "A Review of Nuclear Based Techniques for Cargo Inspection," *Proc. Contraband and Cargo Inspection Technology Int'l Symp.*, pp. 9-19, Washington, DC, (Oct. 1992).
2. J. C. Overley, "Element-Sensitive Computed Tomography with Fast Neutrons," *Nucl. Instr. Meth Phys. Res.* **B24/25**, pp. 1058-1062 (1987).
3. Z. P. Sawa and T. Gozani, "PFNA Technique for the Detection of Explosives," *Proc. 1st Int'l Symp. on Explosive Detection Technology*, DOT/FAA/CT-92/11, pp. 82-103, Atlantic City, NJ (May 1992).
4. J. W. Meadows, "The Thick-Target ^{9}Be(d,n) Neutron Spectra for Deuteron Energies Between 2.6 and 7.0 MeV," ANL/NDM-124, Argonne National Laboratory (Nov. 1991).
5. M. Drosg and O. Schwerer, "Production of Monoenergetic Neutrons Between 0.1 and 23 MeV; Neutron Energies and Cross Sections," in *Handbook on Nuclear Activation Data*, IAEA Technical Report Series No. 273, pp. 83-162 (1987).
6. D. Feautrier and D. L. Smith, "Development and Testing of a Deuterium Gas Target Assembly for Neutron Production via the ^{2}H(d,n)^{3}He Reaction at a Low-Energy Accelerator Facility," ANL/NDM-122, Argonne National Laboratory (March 1992).
7. *CINDA, An Index to the Literature of Microscopic Neutron Data*, International Atomic Energy Agency, Vienna, Austria.
8. P. F. Rose and C. L. Dunford, "Data Formats and Procedures for the Evaluated Nuclear Data File ENDF-6," BNL-NCS 44945, Revised, Brookhaven National Laboratory (Oct. 1991).

9. V. McLane, C. Dunford and P. Rose, *Neutron Cross Sections, Vol. 2: Neutron Cross Section Curves*, Academic Press, Boston (1988).
10. C. Lederer and V. Shirley, *Table of Isotopes*, 7th Edition, John Wiley and Sons, New York (1978).
11. Z. N. Sawa, "PFN GASCA Technique for Detection of Explosives and Drugs," *Nucl. Instr. Meth. Phys. Res.*, **B79**, pp. 593-596 (1993).
12. P. Shea, T. Gozani and H. Bozorgmanesh,"A TNA Explosives-Detection System in Airline Baggage," *Nucl. Instr. Meth. Phys. Res.*, **A299**, pp. 444-448 (1990).
13. G. Knoll, *Radiation Detection and Measurement*, 2nd Edition, John Wiley and Sons, New York (1989).
14. J. W. Motz and M. Danos, "Image Information Content and Patient Exposure," *Med. Phys.* **5**, pp. 8-22 (1978).
15. L. Grodzins, "Optimum Energies for X-Ray Transmission Tomography of Small Samples," *Nucl. Instr. Meth.* **206**, pp. 541-545 (1983).
16. "MCNP - A General Monte Carlo Code for Neutron and Photon Transport, Version 3A," LA-7396-M, Rev. 2, Los Alamos National Laboratory (Sept. 1986).
17. D. L. Smith, "Covariance Matrices and Application to the Field of Nuclear Data," ANL/NDM-62, Argonne National Laboratory (Nov. 1981).
18. J. Orear, "Least Squares when Both Variables Have Uncertainties," *Am. J. Physics* **50**, pp. 912-916 (1982).
19. E. J. Burge, "Errors and Mistakes in the Traditional Optimum Design of Experiments on Exponential Absorption," *Nucl. Instr. Meth.* **144**, pp. 547-555 (1977).
20. D.L. Smith, "A Least-Squares Computational Tool Kit," ANL/NDM-128, Argonne National Laboratory (April 1993).
21. S. Twomey, *Introduction to the Mathematics of Inversion in Remote Sensing and Indirect Measurements*, Elsevier, New York (1979).
22. B. P. Curry, "Constrained Eigenfunction Method for the Inversion of Remote Sensing Data: Application to Particle Size Determination from Light Scattering Measurements," *Appl. Opt.*, **28**, pp. 1345-1355 (1989).
23. H. E. Martz, S. G. Azevedo, J. M. Brase, K. E. Waltjen, and D. J. Schneberk, "Computed Tomography Systems and their Industrial Applications," *Appl. Radiat. Isot.* **41** No. 10/11, *Int. J. Radiat. Appl. Instrum. Part A*, pp. 943-961 (1990).
24. A. V. Crewe and D. A. Crewe, "Inexact Reconstructions from Projections," *Ultramicroscopy* **12**, pp. 293-298 (1984).
25. A. V. Crewe, D. A. Crewe, and O. H. Capp, "Inexact Three-Dimensional Reconstruction of a Biological Macromolecule from a Restricted Number of Projections," *Ultramicroscopy* **13**, pp. 365-372 (1984).
26. J. C. Overley, "Determination of H, C, N, O Content of Bulk Materials from Neutron-Attenuation Measurements," *Int. J. Appl. Radiat. Isot.* **36**, pp. 185-191 (1985).

DISCLAIMER

DATE
FILMED
12/14/93
END